Electric-field-gradient distribution in vitreous yttrium iron garnet

M. Eibschütz, M. E. Lines, and K. Nassau
Bell Laboratories, Murray Hill, New Jersey 07974
(Received 23 October 1979)

Mössbauer quadrupole splitting (QS) measurements are reported for Fe^{57} in vitreous YIG ($Y_3Fe_5O_{12}$). Electric-field-gradient (EFG) calculations from a computer model of amorphous YIG suggest a distribution $p(|V|)$ of principal EFG components V which peaks at a nonzero value, is asymmetric, and falls off exponentially in the wings. A nonlinear least-squares fit to the QS data using a distribution $p(|V|)$ of Lorentzian lines establishes not only the asymmetry but also the detailed non-Gaussian form of the EFG distribution.

This paper reports the measurement of the Mössbauer quadrupole splitting (QS) of Fe^{57} in the paramagnetic phase of vitreous yttrium iron garnet or YIG ($Y_3Fe_5O_{12}$), and its detailed interpretation in terms of the electric-field-gradient distribution at the iron sites. Although there has for some time been a general recognition[1-3] of the fact that amorphous materials avoid high-symmetry local coordination and produce an electric-field-gradient (EFG) distribution $p(|V|)$ which is not peaked at $V=0$ (even in materials which are highly symmetric in their crystalline phase), the detailed form of this distribution has not been established, to our knowledge, for any amorphous or vitreous material. A recent computer model[4] for amorphous YIG strongly suggests that $p(|V|)$ is asymmetrically distributed about its maximum at $V_M \neq 0$ with an exponential falloff on both sides of the peak. Detailed QS measurements reported here, coupled with a careful nonlinear least-squares computer analysis of the data, has enabled us to refine the model and to obtain what we believe to be an accurate description of the EFG distribution at the iron sites in vitreous YIG.

Vitreous YIG has been prepared using the twin roller quenching technique.[5] Stoichiometric oxides $3Y_2O_3$ and $5Fe_2O_3$ were melted in an iridium crucible in air and squirted out of a pin hole to pass between the rollers with a quenching rate of about 10^7 deg/sec. The product consisted of brittle platelets of maximum dimensions $20 \times 10 \times 0.015$ mm^3 (length × width × thickness) which are deep red and transparent after oxygen annealing at 500 °C and nonmagnetic at room temperature. X-ray diffraction of the transparent platelets gives only weak diffuse scattering. Details on preparation and characterization of the vitreous YIG have been given.[5]

The ^{57}Fe Mössbauer absorption spectra were obtained in a standard transmission geometry with a conventional constant acceleration spectrometer using a ^{57}Co in Pd source. The absorber was a mosaic of small platelets. The room-temperature Mössbauer absorption spectrum is shown in Fig. 2(a). The ME spectrum shows two resonance absorption lines due to the electric field gradient at the iron nucleus. The linewidths are broad (full width at half maximum $=0.65$ mm/sec) indicating the existence of a distribution of electric field gradients. The average values of the quadrupole splitting and the isomer shift (IS) estimated from a sum of two Lorentzians fit are 1.12 mm/sec and 0.31 mm/sec (with respect to iron foil), respectively. The value of the isomer shift indicates that iron is in the Fe^{3+} valence state.

A computer model was constructed[4] for amorphous YIG using a basic method involving the sequential addition of hard spheres[6,7] but with the additional requirement that ions of like charge be separated as far as possible within the basic building algorithm. This latter requirement, essential for materials in which Coulomb forces between charged "ions" are playing an important role, tends to minimize the local Coulomb energy. Using a simple point-charge model the EFG distribution $p(|V|)$ of principal EFG components V at the iron sites was computed in histogram form[4] and is reproduced here in Fig. 1. It strongly suggests that the EFG is not symmetrically distributed about its peak and that the distribution falls off very rapidly (and probably exponentially) in the wings.

In Fig. 2(a) we establish first that the measured QS cannot be represented in detail by a sum of two Lorentians and therefore, as expected, that there is not a unique site for the ferric ion in the glass. In the absence of any specific model the next guess has traditionally been that QS is a symmetric Gaussian distribution of Lorentzians and the best fit to this model is shown in Fig. 2(b). Clearly again the picture is inadequate.

For an EFG distribution $p(|V|)$ we can in general describe the QS doublet line shape $f(z)$ by a distribution $p(|V|)$ of Lorentzian lines in the form

$$f(z) = h \int_{-\infty}^{\infty} \frac{(\frac{1}{2}w)^2 p(|V|)}{(\frac{1}{2}w)^2 + (z-V)^2}\, dV \ , \qquad (1)$$

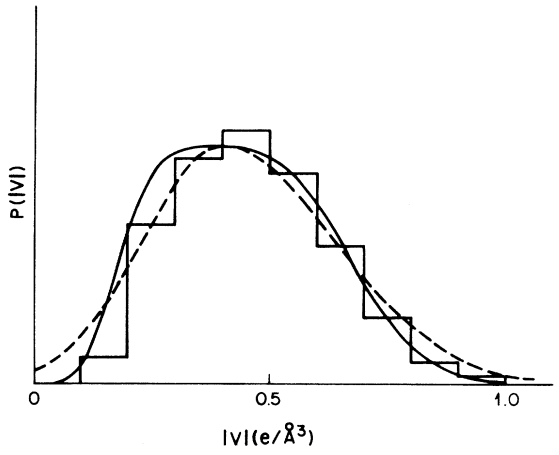

FIG. 1. Histogram of EFG distribution $p(|V|)$ from the computer model calculation of Ref. 4 is compared with the best asymmetric Gaussian (dashed) and asymmetric non-Gaussian (full curve) analytic distributions obtained by use of Eq. (2) with parameters from columns B and D of Table I, respectively.

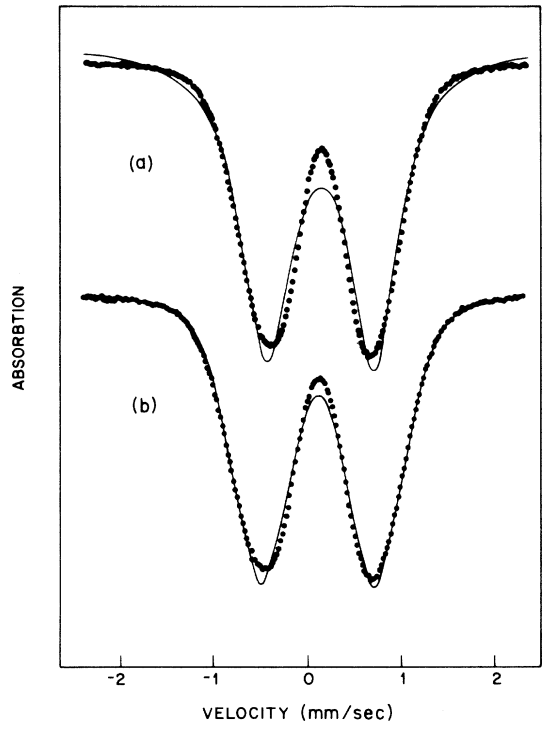

FIG. 2. QS data are compared with the best fit by a pair of Lorentzian lines of arbitrary position, width and height (a) and with the best fit to a symmetric Gaussian distribution of natural width Lorentzians (b), see text, model A.

in which w is the full Lorentzian width at half height, and the amplitude h may differ slightly (h_+, h_-) for the two lines ($V > 0, V < 0$, respectively) as a result of the Gol'danskii-Karyagin effect.[8] However, this effect is usually quite small and we shall discuss the possibility of having $h_+ \neq h_-$ only at the conclusion of the paper.

Led by the computer histogram of Fig. 1 we adopt a general representation for EFG distribution of asymmetric exponential form. Normalized to unity in height it is expressed as

$$p(V) = \begin{cases} p_1(V) = \exp\{-[(V - V_M)/x_1 V_M]^{y_1}\}, \\ \qquad 0 < V < V_M, \\ p_2(V) = \exp\{-[(V - V_M)/x_2 V_M]^{y_2}\}, \\ \qquad V_M < V < \infty, \end{cases} \tag{2}$$

where $V = V_M$ labels the peak of the distribution. This representation allows us to examine in turn the cases A symmetric Gaussian, $x_1 = x_2$, $y_1 = y_2 = 2$, B asymmetric Gaussian, $x_1 \neq x_2$, $y_1 = y_2 = 2$, and finally C asymmetric generalized exponential, $x_1 \neq x_2$, $y_1 \neq y_2 \neq 2$, all within the one formalism. For brevity we shall refer to case C as "asymmetric non-Gaussian".

From Eqs. (1) and (2) the QS doublet is now expressible as

$$f(z) = h_-\left(\int_{-\infty}^{-V_M} F_2\,dV + \int_{-V_M}^{0} F_1\,dV\right) + h_+\left(\int_0^{V_M} F_1\,dV + \int_{V_M}^{\infty} F_2\,dV\right) + B, \tag{3}$$

where

$$F_i = \frac{(\frac{1}{2}w)^2 P_i(|V|)}{(\frac{1}{2}w)^2 + (z - V)^2}, \quad i = 1, 2, \tag{4}$$

and B is a baseline parameter such that $f(z) \to B$ as $z \to \pm\infty$.

Putting the width w equal to the natural Lorentzian linewidth (~ 0.20 mm/sec or, to be specific, 11 channels at 0.0188 mm/sec/channel) the basic model ($h_+ = h_- = h$) contains at most seven parameters, namely h, B, x_1, x_2, y_1, y_2, and V_M. One of these, B, merely defines the zero of the ordinate axis while two others, h and the (peak to peak) quadrupole splitting $\Delta_Q = 2V_M$ set the scales on the two axes. This leaves in general four line-*shape*-determining parameters (x_1, x_2, y_1, y_2) within the model.

In Figs. 2(b), 3(a), and 3(b) we show progressively the least-squares fit of Eq. (2) to the QS data using distributions A to C. The quality of fit can be judged visually or measured quantitatively by the rms deviation parameter ϕ, and the results are summarized in Table I. Although the improvement of fit is mono-

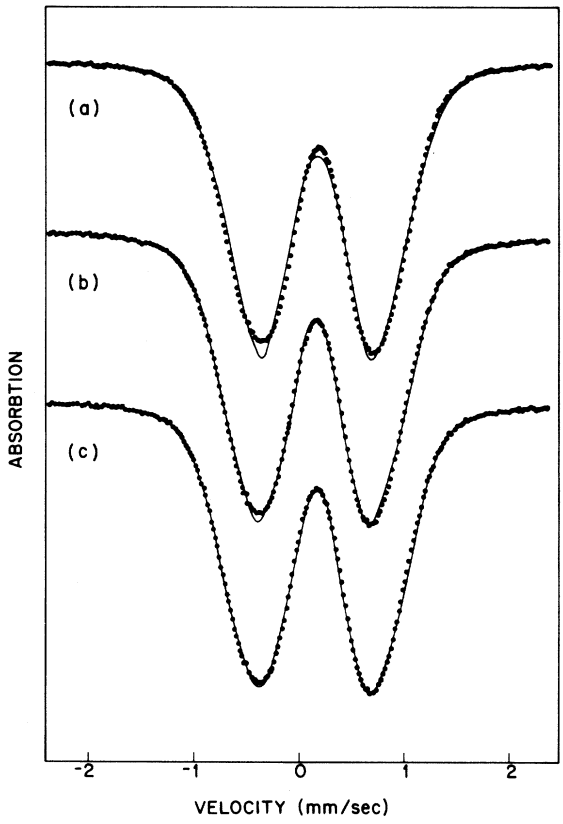

FIG. 3. QS data are compared to least-squares fits using models B [Fig. 3(a)], C [Fig. 3(b)], and D [Fig. 3(c)] of the text.

tonic as we progress from symmetric Gaussian (1 shape-dependent parameter), through asymmetric Gaussian (2) to asymmetric non-Gaussian (4), the dramatic improvement results from the relaxation of the Gaussian restriction. The distribution is undoubtedly asymmetric with $x_2/x_1 \approx 1.3 \pm 0.1$ and the exponents y_1 and y_2 both exceed their Gaussian values of 2, with (model C) $y_1 \approx 3.5$ and $y_2 \approx 2.4$. For none of these cases does a relaxation of the $h = h_\pm$ restriction affect the results significantly ($h_+/h_- \leq 1.015$).

To test the stability of the solution C we have finally allowed both the intensity and linewidth of each of the two (+ and −) sets of Lorentzian constituent lines to float ($h \rightarrow h_+, h_-; w \rightarrow w_+, w_-$). Since this adds three extra parameters this final model (labeled D) in Table I naturally improves the fit to the QS data further, but only by a factor 2 in ϕ, whereas the improvement between B and C was more than a factor 3. The significant finding from model D is that, freely floating, w_+ and w_- adopt values 12.2 and 15.6 channels, respectively, values which are a little larger than the natural width (11 channels) and which therefore are physically realistic. Other parameters are stable to within three standard deviations on floating all variables (going from C to D, Table I) and the values of the exponents y_1 and y_2 tend to deviate even further from the Gaussian value of 2.

In Fig. 1 we sketch the final distribution $p(|V|)$ from D and compare it both with the computer histogram and with the best asymmetric Gaussian approximation of model B. There is a generally impressive agreement with the computer histogram although the

TABLE I. QS model parameters, as defined in the text, determined by nonlinear least-squares fitting to the Mössbauer data. All parameters are dimensionless except Lorentz linewidth w and quadrupole splitting Δ_Q which are measured in units of 1 channel = 0.0188 mm/sec. Numbers underlined are fixed within the model and numbers in parentheses denote errors of one standard deviation or ~70% confidence limits. ϕ is the rms deviation measuring quality of fit.

	A. Symmetric Gaussian	B. Asymmetric Gaussian	C. Asymmetric non-Gaussian	D. All floating (see text)
h_+/h_-	1	1	1	1.19
w	11	11	11	$w_- = 15.6(0.35)$ $w_+ = 12.2(0.36)$
V_M	29.9	27.0	28.3(1.1)	27.8(1.1)
x_1	0.65	0.59	0.65(0.016)	0.60(0.018)
x_2	$=x_1$	0.84	0.79(0.070)	0.80(0.070)
y_1	2	2	3.53(0.27)	4.26(0.39)
y_2	2	2	2.42(0.14)	2.69(0.15)
ϕ	9.02×10^{-3}	4.51×10^{-3}	1.37×10^{-3}	6.47×10^{-4}

latter is not precise enough to reveal the non-Gaussian details of the final solution, or to favor solution D over B except perhaps close to the origin where the computer distribution does appear to fall to zero as $V \rightarrow 0$ faster than the Gaussian distribution.

The unequal amplitudes of the QS peaks, clearly seen from the experimental data, are a reproducible effect. It can only be incorporated into the models discussed in conjunction with an allowance for unequal linewidths as well. Since the Gol'danskii-Karyagin[8] effect alone is unlikely to produce a marked width anomaly, the physical origin of the unequal QS peak amplitudes is still speculative. The unequal widths (as parameterized by $w_+ < w_-$) could, if real, be explained by an inverse correlation between isomer shift and EFG. Since, in the computer model, higher oxygen coordination of an iron correlates with a smaller EFG and since, via additional bonding electron loss from the iron, it may also infer a larger isomer shift, such an effect is physically possible.

In summary we have measured the QS of Fe^{57} in the paramagnetic phase of vitreous YIG and interpreted its line shape using for EFG distribution $p(|V|)$ the refinement of a form suggested by a computer model of YIG. The distribution peaks at a nonzero value, is asymmetric, and is of non-Gaussian form.

We would like to thank G. K. Wertheim for a critical reading of the manuscript.

---

[1]T. E. Sharon and C. C. Tsuei, Phys. Rev. B 5, 1047 (1972).
[2]A. M. van Diepen and Th. J. A. Pompa, J. Phys. (Paris) 37, C6-755 (1976).
[3]G. Férey, A. M. Leclerc, R. de Pape, J. P. Mariot, and F. Varret, Solid State Comm. 29, 477 (1979).
[4]M. E. Lines, Phys. Rev. B 20, 3729 (1979).
[5]E. M. Gyorgy, K. Nassau, M. Eibschütz, J. V. Waszczak, C. A. Wang, and J. C. Shelton, J. Appl. Phys. 50, 2883 (1979).
[6]C. H. Bennett, J. Appl. Phys. 43, 2727 (1972).
[7]See for example R. W. Cochrane, R. Harris, and M. Plischke, J. Non-Cryst. Solids 15, 239 (1974).
[8]V. Gol'danskii *et al.*, Dokl. Akad. Nauk SSSR 147, 127 (1962) [Proc. Acad. Sci. USSR, Phys. Chem. Sect. 147, 766 (1963)]; S. V. Karyagin, *ibid.* 148, 1102 (1963) [*ibid.* 148, 110 (1964).